



17th World Conference on Earthquake Engineering, 17WCEE

Sendai, Japan - September 13th to 18th 2020

DUCTILITY CAPACITY OF COLUMNS AND TOWERS OF TWO SPECIAL BRIDGES

M. C. Gómez-Soberón⁽¹⁾, F. Macal⁽²⁾

(1) Professor-Researcher, Materials Department, Universidad Autónoma Metropolitana, México, cgomez@correo.azc.uam.mx

(2) Post Graduate Student, Universidad Autónoma Metropolitana, México, fabian.macal@hotmail.com

Abstract

Special bridges are structures with unconventional constructive procedures, elements or structural configurations, such as arch, cable-stayed or segmental bridges. Designers of special bridges have to define the ductility capacity in the two directions of analysis, but usually they do not have much experience and there are no recommendations in regulations for all types of bridges.

To enhance the knowledge of the capacity of ductility levels for columns and towers in special bridges, two special bridges were studied. The first bridge is a frame type RC box girder with two inclined columns and two vertical columns, the highest column has 115 m; the width of the slab of the box girder is 13 m and its height varies from 5 m in the midspan to 12 m in the bottom span, with a total length of 528 m. The second bridge is a mixed type, cable-stayed and continuous girders, with two towers (127 m in height), a 400 m in length central span between the towers, two continuous spans of 136 m each, two straight columns of 18 m in height and a total length of 675 m; the columns and towers are hole section. The first bridge configuration was proposed for preliminary designs of real cases and second bridge is an unbuilt project. For these structures the designs of columns and towers were made assuming the location of the structures in different seismic hazardous zones of Mexico.

Based on designs of columns and towers and the structural configuration of bridges, Civil Midas models were developed to perform Standard Pushover Analysis (SPA), Modal Pushover Analysis (MPA) and Non-Linear Response History Analysis (NL-THA); for the last type of analyses ten seismic records were generated for the location the structures, for a characteristic seismic scenario. Specifically, the seismic scenario considered was an earthquake of magnitude 8. For the definition of the nonlinear models, it was taken into account the effective stiffness, the concrete confinement, the P- Δ effects and the distributed plastic hinges were used for the two nonlinear analyses. Capacity of ductility and average demand of ductility (for the ten values) were determined for columns and towers, considering these elements as the only ones having inelastic behavior in the studied models.

The ductility values obtained were compared between the two types of nonlinear analysis in order to conclude if the modal nonlinear static analysis is appropriate to determine the capacity of ductility for bridge elements, because some researchers [1] recommend studying the application MPA in bridge with special structural configuration. In addition, recommendations of ductility capacity values are commented for the types of special bridges studied.

Keywords: special bridges, seismic behavior, ductility capacity, modal pushover analysis



1. Introduction

The special bridges are all those that are not common, those having significant length, special elements, or exceptional characteristics; they are basically different from viaduct, simply supported or continuous bridges. The special bridges have been less studied in the analysis of their behavior and design for external loads, so it is important to expand the knowledge for their best conception.

Recently, some partial or total collapses were reported in special bridges. For example, in 2018 one of the towers of the Chirajara Bridge in Colombia collapsed due to a design error in the resistance of the concrete wall of the tower and the union with the head girder [2]. Also, a pedestrian bridge in Florida (USA), a combination of RC truss and cable-stayed bridge, collapsed during construction due to a poor design of the connection between two members of the truss connected to the slab [3]. In August in Genoa, Italy, a section of the Morandi cable-stayed bridge collapsed, it was based on RC double V towers, RC slab and only two braces covered with reinforced concrete on each side of the towers; it failed because an inadequate maintenance of the braces [4].

As a result of dimensional characteristics in special bridges, only few experimental studies had been performed. Yeh *et al.* [5] conducted real-scale experimental tests of three rectangular piers of hollow RC section, subjected to cyclic excitation. The piers, with length between 3.5 m to 6.5 m, presented ductility between 4.1 and 10.3 with bending or shear faults. Schoettler *et al.* [6] performed the real-scale test of a RC circular pier on the shaking table. The pier of 1.22 m diameter, 7.32 m high above the foundation and 1.55% longitudinal percentage of steel was subjected to ten simulations of records from different stations corresponding to the Loma Prieta and Kobe earthquakes, developing ductility between 0.69 and 8.41. Yi *et al.* [7] conducted an experimental study of a cable-stayed bridge at 1:20 scale, subject to the accelerogram recorded at TCU052 station of the 1999 Chi-Chi earthquake, the original signal was scaled also 1:20 with various intensities. Although its main objective was to evaluate the effect of torsion on the columns of the towers, they also reported results on ductility, so for greatest magnitudes a maximum ductility of approximately 2.8 was registered; unfortunately it was obtained from a mathematical model.

There are more analytical studies for bridges. Ayala [8] estimated the ductility of common bridges, varying some parameters, such as: height of columns (5 m, 10 m and 20 m), number of columns by bent (one and three), cross-sectional shape (wall type, oblong and hollow circular), amount of longitudinal steel (between 1% and 4%) and transverse steel (confined or not), with and without considering the effective stiffness (0 and 50% of the gross inertia), with and without second order effects and considering soil-structure interaction (soft, medium and hard soils). Ductility obtained using static nonlinear analysis varied from 1.10 to 8.72 in the transverse direction, while using nonlinear dynamic analysis the average demand of ductility was 3.09 in the same direction. Raseta *et al.* [9] evaluated the seismic performance of a RC bridge using nonlinear dynamic analysis, the length of the bridge was 170 m, with columns at its base and with different heights (7 m, 14 m, and 21 m), cross section of 5 m long and a width that varies between 1.7 m to 0.5 m. The superstructure was composed of a hollow section of 13.2 m wide and a 4.27 m high. Three real accelerograms were used for the nonlinear dynamic analysis, scaled to be consistent with the elastic spectrum. The obtained ductility was between 3.57 to 3.85 in the longitudinal direction and 1.56 to 1.86 in the transverse direction. Kappos *et al.* [10] implemented the modal nonlinear static analysis in the nonlinear study of the Krystallopigi Bridge, it has a strong angle of curvature in plan, twelve spans with a total length of 638 m, a RC box 13 m wide superstructure and RC hollow rectangular piers with varying heights between 11 m to 27 m. In this structure, three types of analysis were performed: pushover, modal pushover and nonlinear dynamic; formed with synthetic accelerograms compatible with the design spectrum according to Greek regulations. From results, it was determined that the displacements obtained with the static methods are generally smaller than those calculated with the dynamic method.

From what has been previously commented, it is considered necessary to expand the study of the nonlinear behavior of special bridges, since their construction and design is increasingly common. In this work, the capacity and demand of ductility in columns and towers of two special bridges were determined by



means of Standard Pushover Analysis (SPA), Modal Pushover Analysis (MPA) and Non-Linear Response History Analysis (NL-THA).

2. Selected bridge structures

This section describes the main characteristics and general dimensions of the two bridges selected for the study, a RC frame bridge and a mix structure formed by a cable-stayed subsystem and a simple supported section. Also the bridges mathematical models made in the Civil Midas [11] program are explained.

2.1 Frame bridge

The first bridge is a RC frame type, with a total length of 529 m divided into five spans (106 + 195 + 106 + 68 + 53 m); the highest column has a length of about 115 m. The general dimensions of the structure are shown in Fig. 1. The superstructure is a box section with parabolic variation high of 5 m to 12 m along the bridge, except between columns No.4 and No.6 where the section becomes constant. The slab is segmented into 5 m dowels. The substructure includes two inclined columns (No.2 and No.3) monolithically attached to the superstructure and two vertical cantilevered columns, which are attached to the superstructure by sliding supports that allow longitudinal sliding of the slab and restrict it transversely. The four columns have variable sections.

The frame bridge design was carried out in accordance with Mexican regulations [12], with percentages of steel between $\rho = 0.0109$ and $\rho = 0.0123$. For the vertical reinforcement three main branches of #4@0.1 m were supplied and a secondary stirrup of #4. In addition, the design of the superstructure was made to obtain the prestressing strands in order to include them in the mathematical model; their calculation was based on the Mexican Institute of Post-tensioning Manual [13]. The wind action and concrete contraction were not considered, nor the loads of the superstructure design (like braking force, collision, etc.), since they are not within the scope of this work. A ductility capacity of 2 was considered in the design process.

The structural model is based on the one used for the Kochertal Bridge [14]. Specifically, columns were modeled with bar elements and were considered as embedded in their base, so the soil-structure interaction effect was not considered. In addition, the columns were discretized in lengths equal to the theoretical plastic length (in high columns the literature recommends discretizing at least eight sections [15]), for these case 12 sections were obtained for each columns. Columns No.2 and No.3 are connected directly to the slab elements, while the columns No.4 and No.5 are connected by a link element, releasing the degrees of freedom of displacement in the longitudinal direction and its three rotations [16], in order to allow sliding between columns and the slab, simulating a Teflon POT sliding support. The longitudinal movement of the bridge is limited at the extremes by means of springs, simulating a seismic stop based on laminated elastomers or POT type. Fig. 2 shows the model of the bridge made in the Civil Midas program [2], the plastic zones are indicated in red color. To simulate that the slab behaves like a rigid body in the longitudinal direction, the slab nodes were constrained to the node of the gravity center. Two models were developed, in the first one, PRTC01, the effect of degraded inertia was taken into account by multiplying the gross inertia of the columns by 0.7 according to Mexican regulations [12]. In the second model, PRTC02, this effect was considered using the concept of effective stiffness (EI_e) [17] described by Eq. 1.

$$EI_e = M_{yi} / \Phi_{yi} \quad (1)$$

where M_{yi} and Φ_{yi} represent the moment of creep and curvature, respectively; obtained from an idealized moment-curvature bilinear diagram with the axial load acting in the section, without factoring. Because it is a RC structure, a damping value of 0.05 was considered.

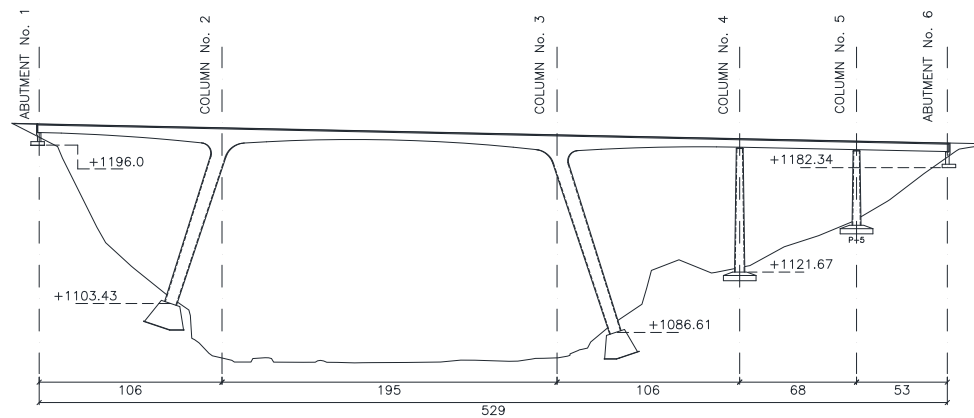


Fig. 1 – General dimensions of the frame bridge

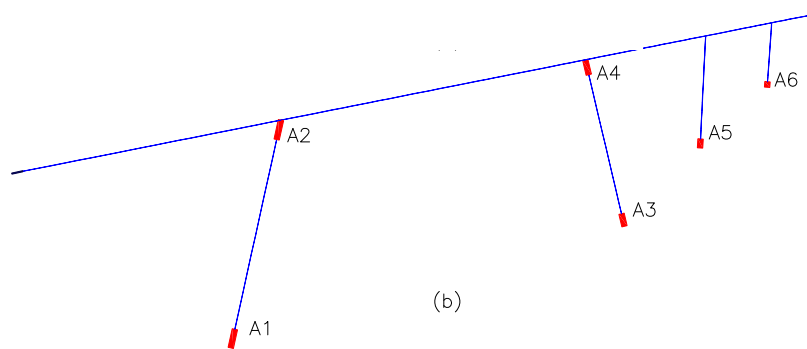


Fig. 2 – Midas Civil frame bridge model

2.2 Cable-stayed bridge

The second selected structure is a cable-stayed bridge of three spans, the main span has 400 m and the lateral spans are of 48 m and 122 m; a total the length of the bridge is 675 m. The approximate height of the towers is 121 m and for piles No.4 and No.5 their lengths are 19 m, including foundation. The general dimensions of the cable-stayed bridge are shown in Fig. 3. The configuration of tower No.2 and No.3 is frame type [15]. The towers start tilted, but once they pass the slab level they become vertical. The first and second section of the tower are variable, the third section becomes constant with thicknesses that vary from 0.75 m to 0.35 m minimum. The vertical elements of the towers are connected to a head girder, which supports the bridge deck, and upper girders that provide stability to the towers. For the structure, a concrete with $f'_c=24.52$ MPa and ASTM-615 reinforcing steel with $f_y=412$ MPa is specified. The percentage of longitudinal steel varies from 4.2% to 4% in the first two segments, and from 3.9% to 2.85% in the third. The deck is formed by structural steel and RC 0.20 m thickness slab. The main beam has a web height of 2.13 m, width of lower and superior flanges of 0.7 m and 0.6 m. Also the thickness of the upper flange varies from 0.051 m to 0.076 m along the bridge, while the thickness of the lower one remains constant with 0.051 m. In the slab a resistance $f'_c=29.42$ MPa is specified, and the main beam is based on structural steel A-709 grade 50 with $f_y=344.7$ MPa. The bridge braces have a fan-type arrangement and are composed of 7-wire strands of 0.0157 m diameter ASTM A-416 steel, with $f_y=1675$ MPa. The area of the wires varies from 0.0013 m² to 0.0058 m² maximum, as well as the pretension force varies from 7.865X10⁵ N to a maximum of 3.5x10⁶ N. On the two towers, deck rests on POT Teflon type supports, which allow a sliding in the longitudinal direction and



restrict them in the transverse direction. On the abutment No.6 the deck sits on Neoprene supports with dimensions of 0.60x0.40x0.057 m. On the other hand, in the abutment No.1, the main beams of the deck are embedded in the dead anchor of the braces at the beginning of the first section.

Towers and columns were modeled with bar elements, as well as the main beam, while the slab was modeled with plate elements. Cables were modeled with the Civil Midas [11] option to model cable type elements, which automatically takes into account the geometric nonlinearity of these elements. In general, the model was based on the recommendations of [18]. The main beams of the left end are embedded according to the construction details, and at the right end, link type elements with the equivalent stiffness of the neoprene support were used. The POT Teflon supports have been modeled with link type elements, which have been provided with an infinite rigidity in the vertical and transverse direction, allowing longitudinal sliding. In general, according to research, the damping in cable-stayed bridges is quite low; in this work a 1% damping was used [19]. Fig. 4 shows the mathematical model made in Civil Midas.

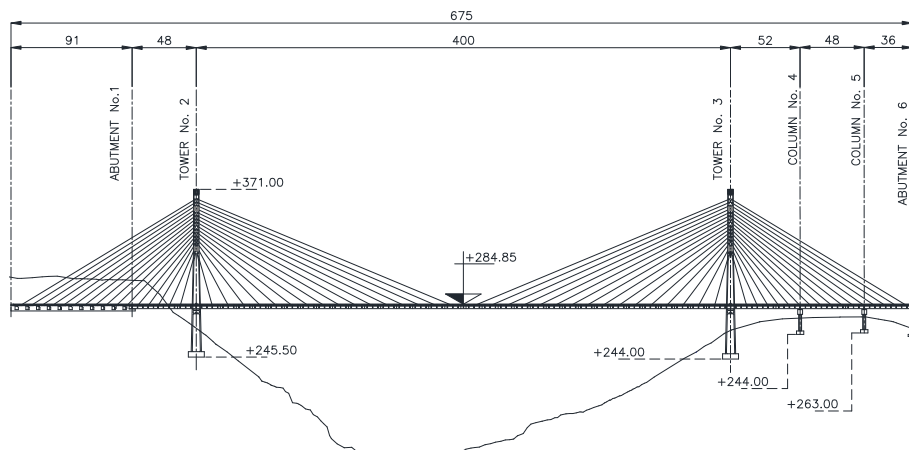


Fig. 3 – General dimensions of the cable-stayed bridge

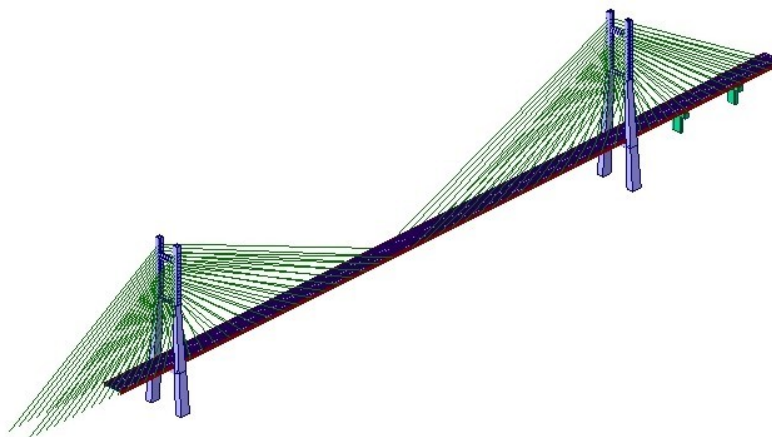


Fig. 4 – Midas Civil mathematical model of the cable-stayed bridge

For these structures two models were also considered, in the first, ATRNTD01, the inertia of the columns and beams of towers and columns were multiplied by a factor. Beams were affected by $0.5I_g$ and



columns by $0.7I_g$ [12]. For the second model, ATRNTD01, the effective inertial was applied using the criteria [17]. For the towers the averages factors were between 0.67 and 0.88. In columns No.4 and No.5, values were of 0.33 and 0.3, while in the girder heads was 0.5. Deck and other elements have been considered elastic, since they have few contributions in resistance to lateral loads.

3. Seismic load characterization

The studied bridges were designed for their construction in different locations, so the seismic hazard used is also different. In the case of the frame bridge, to obtain displacement demand using the MPA, the elastic spectrum shown in Figure 5 (left) was used [19]. In order to perform the nonlinear dynamic analysis, twelve accelerograms registered in México [20] were selected, these were corrected by baseline and filtered; their characteristics are shown in Table 1.

Elastic spectrum used for the cable-stayed bridge is shown in Fig. 5 (right). The accelerograms used in the nonlinear dynamic analysis of this bridge were taken from similar seismic zones, since there was insufficient information for the proper location of the structure. The characteristics of the used earthquakes are indicated in Table 2. In Fig. 6, the elastic spectrums are shown, with damping of 5%, of the stronger horizontal component of the selected accelerograms for the two bridges.

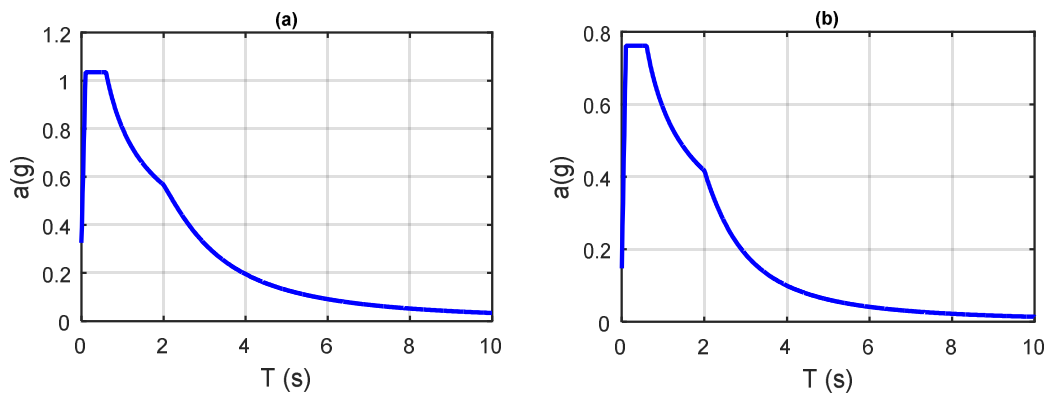


Fig. 5 – Used elastic spectrums, left for the frame bridge and right for the cable-stayed bridge

3. Analyses and results

For each of the bridges under study, three types of analysis were performed: standard pushover (SPA), modal pushover (MPA) and dynamic nonlinear (NL-THA). For the last one, accelerograms presented in the previous section were used, averaging the obtained values. From results, the transverse direction is analyzed because it is the most critical, and the ductility obtained for different levels of performance is reported.

3.1 Frame bridge

For standard nonlinear static analysis the transversal ductility corresponding to the performance levels of immediate occupancy (IO), life safety (LS) and collapse prevention (CP) for the PRTC01 model are 1.61, 1.90 and 2.20 respectively, while the maximum value (just before starting the fall of the shear force vs displacement curve) is 2.83. For the PRTC02 model these values are 1.27, 1.41 and 1.54 for IO, LS and CP performance levels and 2.85 for the maximum value.

Table 3 shows the characteristics of the principal mode shapes of the PRTC01 and PRTC02 models with their respective percentage of modal mass participation, used in MPA. Analyzes considered as many modes as necessary to obtain 90% of the effective mass. The greatest difficulty in static modal analyzes was to define the monitoring point, since it is not the same for all modes, so it could be observed from the one at



the top of the columns that provides stable curves of shear force vs. displacement. Applying the MPA [21], the total response is obtained by modal combination, so in the last column of Table 3 the demands ductility of each mode and models are shown. Total ductility is obtained using the SRSS modal combination rule, determining a value of 1.88 and 1.37 for PRTC01 and PRTC02 models, respectively.

Table 1 – Accelerograms used for the dynamic analysis if the frame bridge

State	Station name	Clave	Date	Magnitude	a_{max} (gals)
Michoacán	Apatzingán	APAT	14/mar/1979	7.0	62.217
Michoacán	Apatzingán	APAT	25/oct/1981	7.3	96.548
Michoacán	Apatzingán	APAT	19/sep/1985	8.1	81.282
Michoacán	Asteaga	ARTG	30/abr/1986	7.0	27.060
Michoacán	Caleta de Campos	CALE	19/sep/1985	8.1	140.680
Jalisco	Chamela	CJIG	30/sep/1999	7.5	0.211
Colima	Colima	COIG	30/sep/1999	7.5	0.747
Colima	Colima	COLI	30/abr/1986	7.0	84.052
Michoacán	Guacamayas	GUAC	30/abr/1986	7.0	55.444
Michoacán	Zacatula	ZACA	19/sep/1985	8.1	262.230
Guerrero	Estación No.1, Acapulco	ACAJ	08/sep/2017	8.2	15.430
Guerrero	Estación No.1, Acapulco	ACAJ	19/sep/2017	7.1	3.370

Table 2 – Accelerograms used for the dynamic analysis of the cable-stayed bridge

State	Station name	Clave	Date	Magnitude	a_{max} (gals)
Puebla	Parque Habana	PHPU	08/sep/2017	8.2	25.12
Villahermosa	Secundaria M Altamirano	VHSA	08/sep/2017	8.2	2.19
Veracruz	Soledad Doblado	SODO	08/sep/2017	8.2	14.19
Veracruz	Laguna verde	LVIG	30/sep/1999	7.6	3.46
Puebla	Popocatepetl	PPIG	30/sep/1999	7.5	22.310
Veracruz	Soledad Doblado	SODO	18/abr/2014	7.2	5.63
Cuernavaca	Estación No.5	CUER	08/sep/2017	8.2	14.32
Cuernavaca	Estación No.5	CUER	19/sep/2017	8.2	161.89
Villahermosa	Secundaria M Altamirano	VHSA	16/feb/2018	7.2	2.67
Guanajuato	Acámbaro	ACAM	16/feb/2018	7.2	2.44

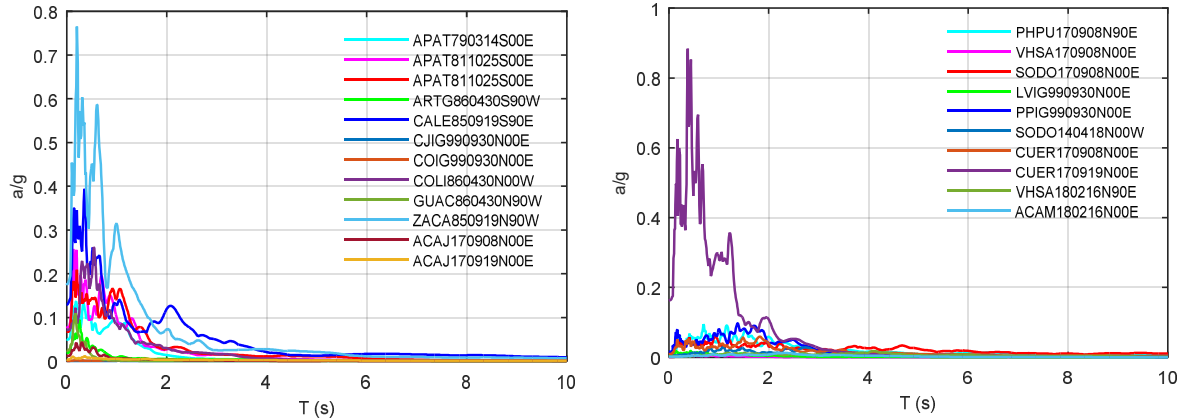


Fig. 6 – Elastic spectrums of the used accelerograms for frame bridge (left) and cable-stayed bridge (right). Strong horizontal component.

Table 3 – MPA results for the frame bridge models

Mode	Period (s)	P long. (%)	P. transv. (%)	Γ_{long}	Γ_{transv}	Nmon	ϕ_{rn}	μ
PTRC01 model								
1	5.400	0	65.95	0	1.43	23	0.66	1.41
3	1.767	0	13.05	0	0.71	157	0.08	0.46
7	0.827	0	4.49	0	0.47	157	0.91	0.90
13	0.487	0	2.89	0	0.64	61	0.14	0.24
16	0.401	0	3.7	0	0.73	157	0.15	0.67
PTRC02 Model								
1	7.913	0	69.79	0	1.39	61	0.87	1.15
4	2.000	0	10.05	0	0.62	144	0.86	0.49
8	0.853	0	4.39	0	0.45	157	0.89	0.52
9	0.735	0	2.42	0	0.54	157	0.16	0.16
13	0.574	0	1.36	0	0.46	23	0.15	0.13
17	0.474	0	3.25	0	0.79	157	0.04	0.07
Γ = modal participating factors; Nmon =monitoring node; ϕ_{rn} =modal value of Nmon, μ =ductility								

For the nonlinear dynamic analyses, accelerograms indicated in previous sections were used. Each accelerogram was affected by a factor, whose value is calculated by resembling the spectral ordinates of the register and the design spectrum for the transversal first period of the structure; the average values for models PTRC01 and PTRC02 were 2.22 and 0.96, respectively.



The results of the total displacements obtained with the SPA, MPA and the average displacements of the NL-THA, were compared, as it is shown in Fig. 7. The solid lines correspond to the PRTC01 model and the dashed lines correspond to the PRTC02 model; it is observed in both cases that the PA estimates and covers very well the displacement of columns No.2 and No.3 (the highest columns), but did not have good accuracy with columns No.4 and No.5. The MPA also has a good precision to calculate the displacement of columns No.2 and No.3 compared to the NL-THA, however there is no good precision in columns No.4 and No.5. In particular the PRTC02 model, in MPA, has a very good approximation in columns No.2, No.3 and No.4, including that displacement of column No. 3 is underestimated.

3.2 Cable-stayed bridge

For the standard pushover analysis, ductility values of 3.09, 3.49, 3.87 and 4.27 for IO, LS and CP performance levels and the maximum value, respectively, were determined with SPA for the ATRND01 model. The same values for the ATRND02 model were of 2.50, 2.83, 3.13 and 3.13. To develop the MPA, the dynamic properties of models ATRND01 and ATRND02 were defined. The characteristics of the first and used modal shapes are described in Table 4, where the ductility obtained in each mode is also indicated in the last column. These values are combined by SRSS and CQC rules, obtaining ductility values of 1.96 and 2.21 for the ATRND01 model and 1.79 and 1.97 for the ATRND02 model. Accelerograms selected for the location of the cable-stayed bridge were also scaled as it has previously commented. After that, the structure was subjected to these records and the ductility values of each record were defined, to obtain the ductility averages of 2.17 and 2.13 for models ATRND01 and ATRND02, respectively.

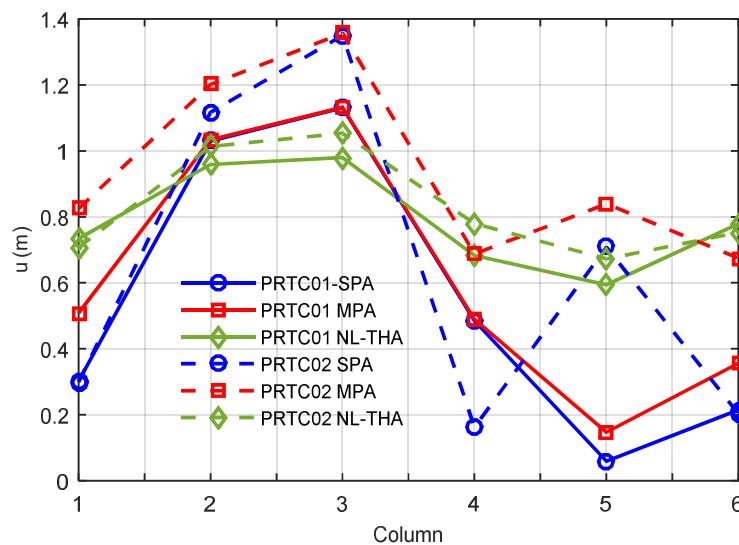


Fig. 7 – Total displacement obtained with different analyses and models. Frame bridge

Figure 8 presents the displacements at the upper end of the towers and columns for each type of analysis. It shows how the CQC of the MPA is the one with the best prediction of the displacements compared to the NL-THA for the case of the ATRNTD02 model, and for the ATRNTD01 neither MPA-SRSS nor MPA-CQC have good accuracy. In both cases, greater displacements were obtained in the NL-THA than in the SPA and MPA. Regarding to the ductility demand using the MPA, the results obtained appear to be consistent, since for the second model the ductility was reduced, because the bridge became slightly more flexible. However, in the MPA it was 10% down compared to the ductility obtained using the first model NL-THA, and it was 19% lower for the second model.



Table 4 – MPA results for the cable-stayed bridge models

Mode	Period (s)	P long. (%)	P. transv. (%)	Γ_{long}	Γ_{transv}	Nmon	ϕ_{rn}	μ
ATNRTD01 model								
2	5.400	0	31.81	0	1.75	80	1.00	1.29
3	2.131	0	5.91	0	0.77	40	1.00	0.80
5	2.090	0	1.35	0	0.52	40	0.12	0.06
9	1.722	0	2.24	0	0.60	40	0.08	0.10
12	1.026	0	15.65	0	1.32	40	0.55	0.88
18	0.617	0	21.30	0	0.89	40	0.62	0.83
24	0.52	0	1.98	0	-0.48	379	0.063	0.14
38	0.336	0	5.77	0	1.14	385	0.080	0.10
39	0.323	0	4.34	0	1.37	385	0.052	0.14
ATNRTD02 model								
2	2.083	0	32.07	0	1.80	80	1.00	1.29
3	2.024	0	7.54	0	0.91	40	1.00	0.80
9	1.028	0	2.47	0	0.64	40	0.08	0.06
14	0.742	0	20.66	0	1.40	40	0.45	0.10
17	0.681	0	2.28	0	0.58	40	1.00	0.88
20	0.611	0	15.99	0	1.02	80	0.17	0.83
38	0.337	0	5.38	0	0.96	379	0.11	0.14
39	0.324	0	2.90	0	1.18	385	0.09	0.10
Γ = modal participating factors; Nmon =monitoring node; ϕ_{rn} =modal value of Nmon, μ =ductility								

4. Final commentaries

To define the ductility of two types of special bridges (frame and cables-stayed) mathematical models were elaborated to develop standard pushover, modal pushover and dynamic nonlinear analyses. Ductility values defined with pushover analyses were compared with the average demand ductility for ten representative accelerograms in each bridge location, obtained with nonlinear dynamic analyzes. For each studied bridge, two models were considered, depending on the definition applied to take into account the degraded inertia, with the Mexican regulation proposal $0.7I_g$ and the effective stiffness, αI_g ; where I_g is the gross inertia of the section. Depending on the formulation, the inertia changed between $0.3I_g$ and up to $0.85I_g$, which could generate very different structural models in terms of their dynamic properties.

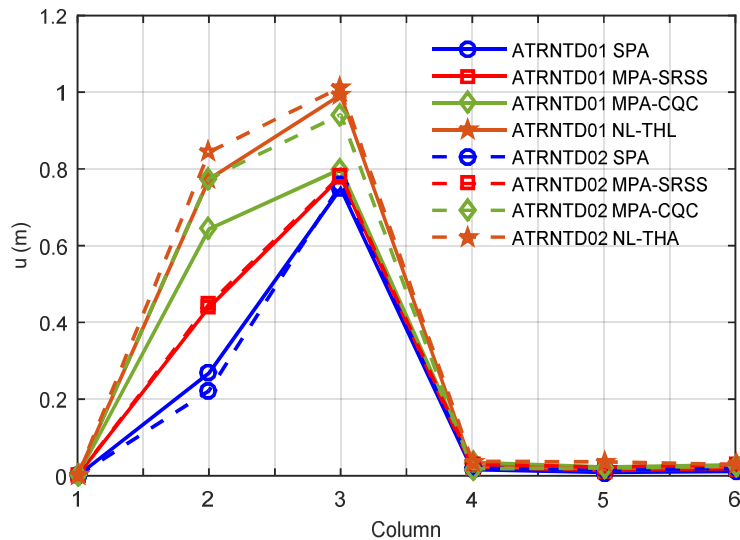


Fig. 8 – Total displacement obtained with different analyses and models. Cable-stayed bridge

From results, general conclusions are:

- In this work the columns and towers of the bridges were designed using gross inertia, because it is not clear which value of degraded inertia should be used. This action represents a conservative design.
- A ductility of two is recommended in literature for common frame bridge columns. In the studied bridges, similar values to this proposal were obtained in the PRTC01 model, but lower values for the PRTC02 model; with all types of analysis. Ductility values of the PRTC01 model approximate a CP performance level, while for the PRTC02 model it would be a LS performance level. Then, depending on the factor by which the inertia of the structural elements is affected, very different responses would be defined. It is considered that if this factor is 0.3 there are unreal conditions.
- For the frame bridge there are greater differences in the displacements at the end of the columns when using SPA or MPA, and NL-THA procedures (Fig. 7), although these differences are not so visible in ductility values. So, for this bridge it is not recommended to use the SPA or MPA; although this conclusion should be ratified with further analysis in bridges with a similar typology.
- For the cable-stayed bridge, the displacements obtained with the MPA were lower than the NL-THA averages, with differences of up to 25%. Therefore, the approximate method underestimates the displacements. In ductility values the differences were not so great, with maximum values of 10% and 19% for the ATRNTD01 and ATRNTD02 models.
- In general and for the studied bridges, the SPA is easy to apply but does not match the results obtained with rigorous methods. The MPA are initially difficult to understand, their practical application is restricted because they are not usually included in commercial analysis programs and take less calculation time; also they provide a good estimate of ductility values but may underestimate maximum displacements, compared to rigorous methods.

These conclusions must be ratified with further analysis in similar o different typologies of special bridges.



17th World Conference on Earthquake Engineering, 17WCEE

Sendai, Japan - September 13th to 18th 2020

5. Acknowledgements

Authors would like to thank Conacyt for partially sponsoring this project with the second author graduate scholarship. The companies MEXICANA DE PRESFUERZO S.A. C.V. and CARLOS FERNÁNDEZ CASADO S.L are also thanked for providing previous designs of the two studied bridges.

6. References

- [1] Paraskeva TS, Kappos AJ, Sextos AG (2006): Extension of modal pushover analysis to seismic assessment of bridges. *Earthquake Engineering and Structural Dynamics*, 35, 1269-1293.
- [2] Coviandes SAS (2018): Boletín de prensa especial. Bogotá, Colombia: Concesionaria Vial de los Andes-Coviandes SAS <https://www.researchgate.net>
- [3] FHWA (2018): Investigation HWY18MH009: Pedestrian bridge collapse in construction, Miami, Florida. Federal Highway Administration. <https://highways.dot.gov/>.
- [4] Pollock E (2018): Italy's Morandi Bridge Collapse-What Do We Know?. Toronto, Canada. Engineering. <https://www.engineering.com/>.
- [5] Yeh YK, Mo YL, Yang CY (2002): Seismic Performance of Rectangular Hollow Bridge Columns. *Journal of Structural Engineering*, 128 (1), 60-68.
- [6] Schoettler MJ, Restrepo JI, Guerrini G, Duck DE, Carrera F (2015): A full-scale, single-column bridge bent tested by shake-table excitation. Technical Report No. 2015/02, Pacific Earthquake Engineering Research Center..
- [7] Yi J, Li J (2019): Experimental and numerical study on seismic response of inclined tower legs of cable-stayed bridge during earthquake. *Engineering Structures*, 183, 180-194.
- [8] Ayala A (2016): Estudio paramétrico de la demanda de ductilidad en pilas de puentes comunes. Universidad Autónoma Metropolitana, Structures Postgraduate Program, Master Thesis, Ciudad de México, México.
- [9] Raseta A, Ladinovic D, Radujkovic A (2017): The estimation of seismic performances of reinforced concrete girder bridges using nonlinear dynamic analysis. *Tehnicki vjesnik*, 24 (2), 489-496.
- [10] Kappos, A J, G D Manolis y I F Mochonas (2002). "Seismic assessment and design of R/C bridges with irregular configuration, including SSI effects" *Engineering Structures* 24, 1337-1348.
- [11] Midas Civil (2019): A higher standard of bridge design. MIDASoft, Inc.
- [12] NTCC-2017 (2017). Normas Técnicas Complementarias para Diseño y Construcción de Estructuras de Concreto. Ciudad de México, México: Gaceta Oficial del Distrito Federal. Mexican regulations, in Spanish.
- [13] PTI (2006): Post-Tensioning Manual/Sixth Edition. Arizona, Estado Unidos: POST-TENSIONING INSTITUTE.
- [14] Leonhard F. (1979): Estructuras de hormigón, TOMO VI: Bases para la construcción de puentes monolíticos. Berlin, Germany: Springer. Spanish traduction.
- [15] Manterola J (2006): Puentes: Apuntes para su diseño, calculo y construcción. Madrid, Spain. Colegio de Caminos, Canales y Puertos.
- [16] CALTRANS (2019): Seismic design criteria. California, Estados Unidos: California Department of Transportation.
- [17] Priestley M J N, Calvi G M (1996): Seismic design and retrofit of bridges. New York, USA: John Wiley & Sons, Inc.
- [18] Fu C, Wang S (2015): Computational Analysis and Design of Bridge Structures. New York, USA, CRC Press.
- [19] Chen W, Duan L (2014). Bridge Engineering Handbook, Seismic Design. Florida, USA, CRC Press.
- [20] BMSF (2000): Strong Earthquakes Mexican database, CDROOM. Sociedad Mexicana de Ingeniería Sísmica.
- [21] Chopra, A. K. y Goel, R. K. (2001). PEER Report No. 2001/03: A Modal Pushover Analysis Procedure to Estimate Seismic Demands for Buildings. California, Estados Unidos: Pacific Earthquake Engineering Research Center.